ORIGINAL PAPER

Design of Benzene-1,2-diamines as selective inducible nitric oxide synthase inhibitors: a combined de novo design and docking analysis

Sandrea M. Francis · Amit Mittal · Manishika Sharma · Prasad V. Bharatam

Abstract Selective inhibition of inducible nitric oxide synthases (iNOS) has been a challenging problem for researchers pursuing work in finding methods to treat inflammatory disorders, shock, etc. Though many inhibitors have been studied to date, all are associated with selectivity or potency problems. Additionally, most of the reported compounds have several similarities and fewer number of novel structures are being tried. There is an increasing need to design novel molecules for this target. In this work, de novo design using LUDI, combined with docking analysis using FlexX has been employed in an attempt to identify novel scaffolds. Benzene-1,2-diamines were identified which could mimic the interactions of the substrate analogs and other inhibitors. Comparative docking scores in each of the isoforms of nitric oxide synthase were employed to recognize hits for iNOS selectivity.

S. M. Francis · M. Sharma
Department of Pharmacoinformatics, National Institute
of Pharmaceutical Education and Research (NIPER),
Sector-67, S.A.S. Nagar,
160 062 Punjab, India

A. Mittal
Department of Pharmaceutical Technology, National Institute
of Pharmaceutical Education and Research (NIPER),
Sector-67, S.A.S. Nagar,
160 062 Punjab, India

P. V. Bharatam (✉)
Department of Medicinal Chemistry, National Institute
of Pharmaceutical Education and Research (NIPER),
Sector-67, S.A.S. Nagar,
160 062 Punjab, India
e-mail: pvbharatam@niper.ac.in

Introduction

Nitric oxide (NO), the reactive free radical gas produced in mammalian systems by the enzyme nitric oxide synthase (NOS) is a ubiquitous biomessenger involved in many physiological and pathological processes. Nitric oxide is produced in a two-step, 5-eletron oxidation process by conversion of the natural substrate, L-Arginine (L-Arg) through $N\omega$-hydroxy-L-arginine (NOH-L-Arg) to the final products, L-citrulline and NO [1]. Three principal isoforms of NOS have been identified in mammals which are, the Ca^{2+}/calmodulin regulated constitutive NOS (cNOS) comprising of endothelial NOS (eNOS) and neuronal NOS (nNOS) found predominantly in the vascular endothelium and brain respectively, and the Ca^{2+}/calmodulin independent inducible NOS (iNOS) which is expressed in macrophages and is believed to be involved in host defense mechanism. However, the iNOS isoform is also implicated in several pathological conditions due to the overproduction of NO in response to cytokines or bacterial endotoxin, some of which are chronic inflammatory diseases, asthma, septic shock and rheumatoid arthritis [1, 2, 3]. Appreciation of the pathological roles of iNOS-derived NO has stimulated interest in the design and synthesis of iNOS inhibitors for potential therapeutic use in disorders associated with the overproduction of NO. Though nNOS inhibition is desirable in pathological conditions like stroke, inhibition of endothelial NOS; it is highly undesirable because of its role in the maintenance of cardiovascular homeostasis and so a

search for potent and highly selective iNOS inhibitors is currently an area of intense research.

Nitric oxide synthase isoforms are homodimers, with an N-terminal oxygenase and C-terminal reductase domain comprising of five cofactors, iron protoporphyrin IX (heme), (6R)-5,6,7,8-tetrahydrobiopterin (H4B), NADPH, FAD and FMN, in each monomer. They are large enzymes ranging in size from 130 to 160 kDa and the three NOS isoforms share more than 50–60% sequence identity [4]. However, the high conservation of the heme active site
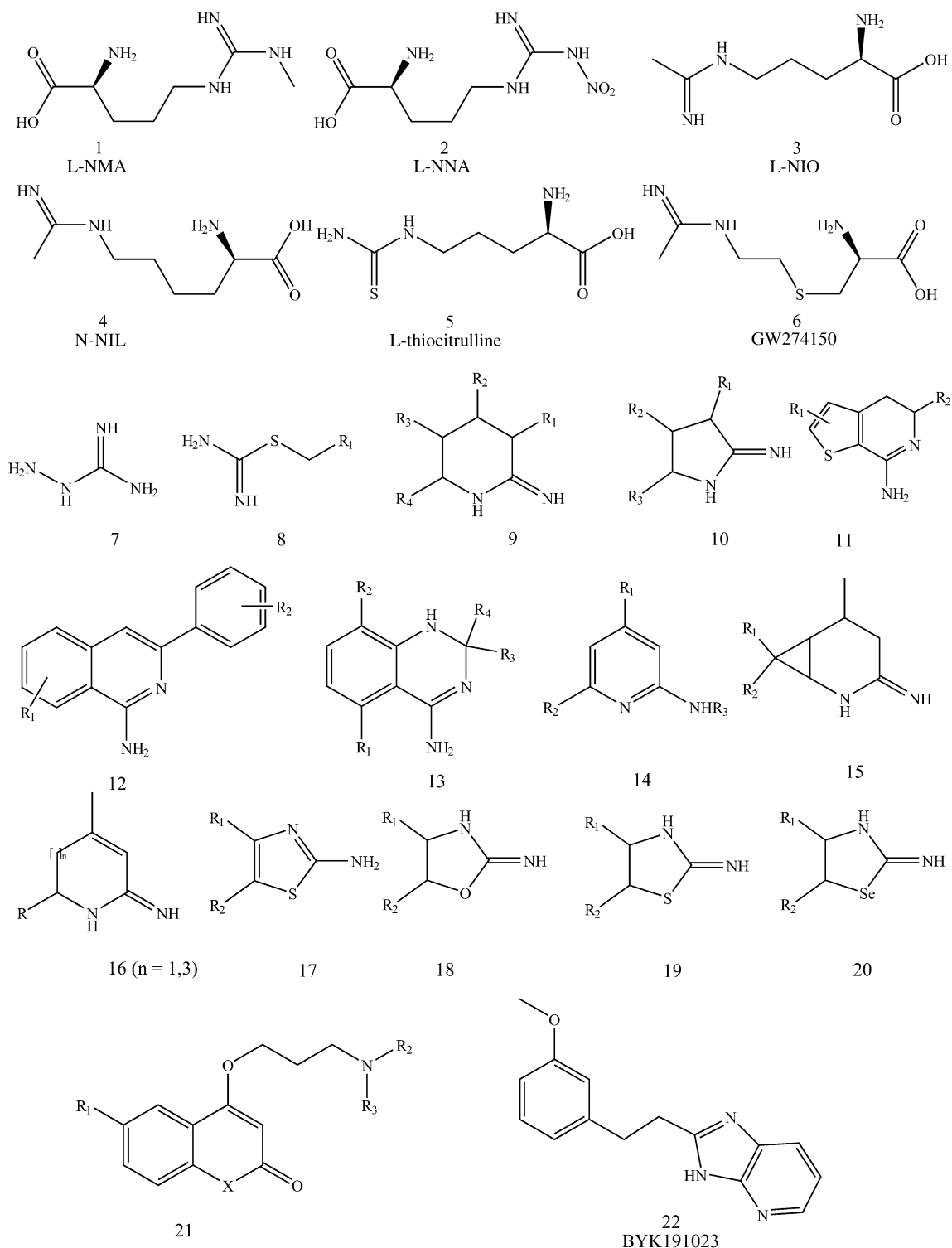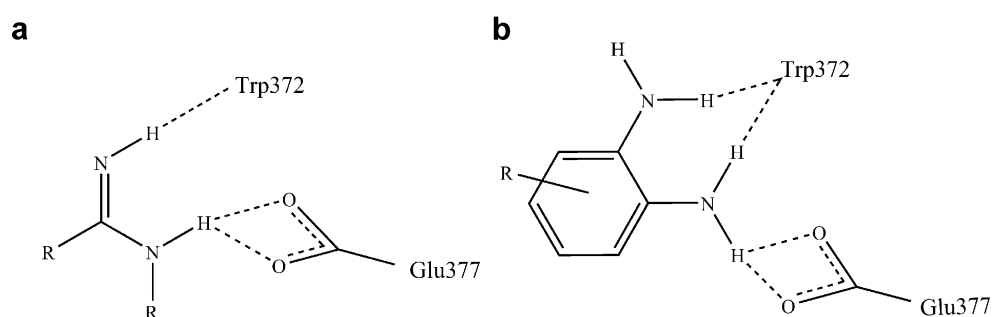

Fig. 1 A selected list of L-arginine analogs and non-amino acid based inhibitors of NOS. Structures 1–6 are L-arginine analogs and 7–22 are non-amino acid based inhibitors

residues revealed by the crystal structures of the oxygenase domains of all three isoforms makes the task of achieving selectivity for iNOS difficult [5, 6]. The active site of NOSs consists of four pockets, the substrate binding S pocket, the middle M pocket, the C1 pocket and C2 pocket in the substrate access channels [7]. The active site has been extensively studied by various research groups [7–12] and the residues Trp372 and Glu377 in the S pocket (iNOS) have been found to be the main residues with which the substrates (L-Arg or NOH-L-Arg) form extensive hydrogen bond network thereby orienting the guanidinium nitrogen above the heme for oxidation. Most of the NOS inhibitors like L-Arg analogues, thioureas, and amidines mimic the L-Arg guanidinium–protein interactions and generally exhibit poor isoform selectivity. The subtle differences that exist above the S pocket and into the substrate access channel can be utilized for the rational design of isoform-specific NOS inhibitors [9].

The NOS inhibitors reported to date includes both the substrate analogs (L-Arg) and non-amino acid based inhib-itors. The L-arginine analogs include N^G-methyl-L-arginine (L-NMA) [1], N^G-nitro-L-arginine (L-NNA) [2], N-(1-imi-noethyl)-L-ornithine (L-NIO) [3], N-(1-imino-3-butenyl)-L-ornithine (L-VNIO), N-(1-iminoethyl)-L-lysine (L-NIL) [4], and L-thiocitrulline [5] etc. The non-amino acid inhibitors belonging to the following classes: aminoguanidine [7], isothioureas [8], 2-iminopiperidines [9], 2-iminopyrrolidines [10], thienopyridines [11], 3,4-dihydro-1-isoquinolinamines [12], 1,2-dihydro-4-quinazolinamine [13], 2-aminopyridines

[14], 2-azabicyclo[4.1.0]heptan-3-imines [15], Dihydropyr-idin-2(1H)-imines and 1,5,6,7-tetrahydro-2H-azepin-2-imines [16], 2-aminothiazoles [17], oxazolidine-2-imines [18], thiazolidine-2-imines [19], selenazolidines-2-imines [20], coumarins [21], imidazopyridines [22] and so on [13–34]. The compound (ONO-1714) (1S,5S,6R,7R)-7-chloro-3-imino-5-methyl-2-azabicyclo[4.1.0]-heptane hydrochloride [35] and S-[2-[(1-iminoethyl)- amino]ethyl]-l-homocysteine (GW274150) [6] [36] have reached clinical trials. Some of the reported L-Arginine analogs and the non amino acid inhibitors are given in Fig. 1.

All these molecules are associated with selectivity, potency, toxicity or bioavailability problems and none have yet made it to the market [35, 37]. Hence a need arises to design novel molecules for this enzyme. Also, conventionally, the guanidine, amidine, thiourea or isothiourea motifs have been accepted to be an essential feature for binding to the guanidinium binding region of the L-Arginine binding site [38]. Aparna et al. have reported a molecular dynamics study providing insights into selectivity of NOS isoforms [39]. Several other workers also employed the structure based design methods to obtain new leads [6, 40–42]. In this study, structure based drug design approaches have been employed to identify molecules with unexplored scaffolds, taking the selectivity factor into consideration. De novo design using the LUDI program and docking methodology using FlexX algorithm were used to identify the rational backbone structure for the combinatorial library generation.
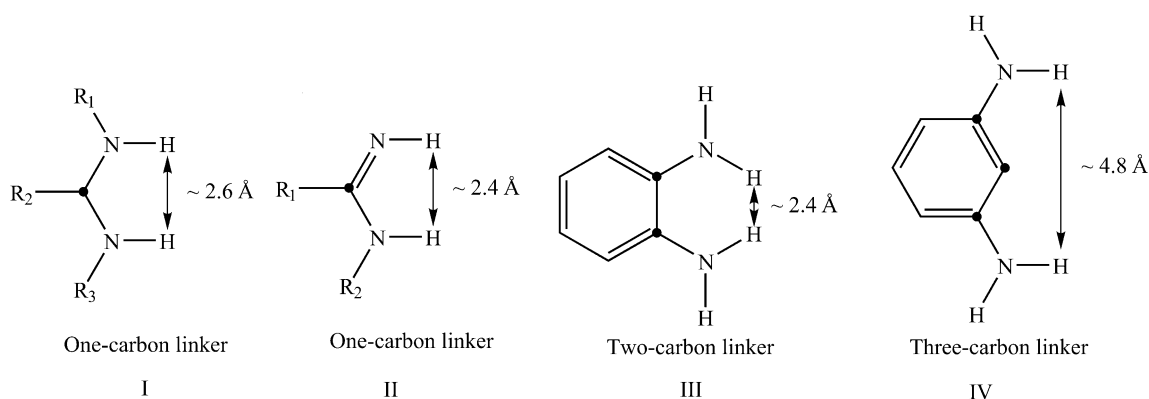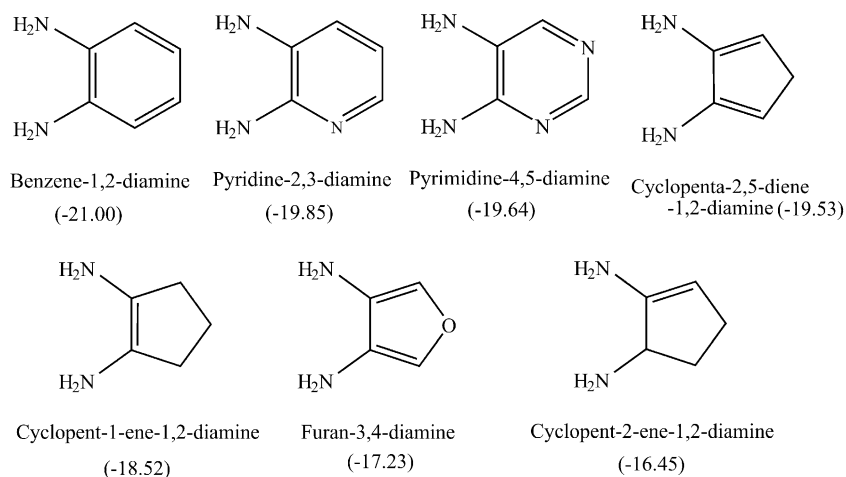

Fig. 3 Fragments with one-, two- and three- carbon linkers (given as dots) between the two nitrogens

Fig. 4 Some of the designed fragments with a two carbon atom linker between the nitrogens which showed the required base interaction with the main residues Trp372 and Glu377. The docking score of the fragment obtained using FlexX are given in brackets

Benzene-1,2-diamine (-21.00)

Pyridine-2,3-diamine (-19.85)

Pyrimidine-4,5-diamine (-19.64)

Cyclopenta-2,5-diene -1,2-diamine (-19.53)

Cyclopent-1-ene-1,2-diamine (-18.52)

Furan-3,4-diamine (-17.23)

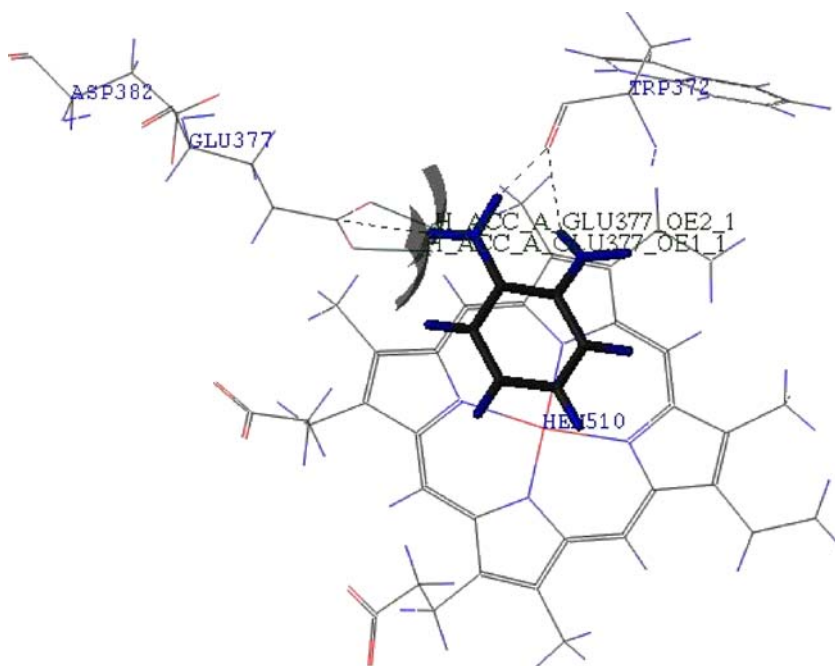Cyclopent-2-ene-1,2-diamine (-16.45)

Computational details

The de novo program used for the study was the fragment based approach LUDI from Cerius2 software package. This algorithm identifies plausible which generates interaction sites and positions suitable fragments from an inbuilt library into the active site based on the following scoring function given by Böhm. The LUDI score is calculated with the free energy of binding (ΔG) expressed by an empirical function (Böhm, 1994) [43].

$$\Delta G = \Delta G_o + \Delta G_{hb} \sum f(\Delta R) f(\Delta \alpha)$$
$$+ \Delta G_{ion} \sum f(\Delta R) f(\Delta \alpha) + \Delta G_{lipo} A_{lipo}$$
$$+ \Delta G_{rot} NR + \Delta G_{aro/aro} \Delta N_{aro/aro}$$

Where ΔG_0 represents the constant contribution to the binding energy due to loss of translational and rotational entropy of the fragment. ΔG_{hb} and ΔG_{ion} represent the contributions from an ideal neutral hydrogen bond and an ideal ionic interaction, respectively. The ΔG_{lipo} term represents the contribution from lipophilic contact and ΔG_{rot} term represents the contribution due to the freezing of internal degrees of freedom in the fragment. NR is the number of acyclic sp^3-sp^3 and sp^3-sp^2 bonds.

About 90 crystal structures of NOS have been solved and deposited in the protein data bank (PDB). The structure reported for human iNOS (PDB id: 4NOS), [9] human eNOS (PDB id: 3NOS (2.40 Å)) [9] and rat nNOS (PDB id: 1OM4 (1.75 Å)) have been employed in this work for de novo design and docking. The protein structures were prepared by checking for consistency and correct atom

Fig. 5 The hydrogen bonding network of benzene-1,2-diamine with Trp372 and Glu377 obtained from LUDI analysis

types in the active site and addition of hydrogen atoms. Definition of the active site, designing and docking was carried out from the 3D structure of "chain A" in all three isoforms. The active site of iNOS is more or less in an inverted pear-shape with the guanidine moiety of substrate occupying the farther end of the site above the heme and its tail part protruding into the middle pocket, substrate access channel. The area around heme in the substrate binding pocket (S pocket) comprising of the main residues Trp372 and Glu377 is small, and not able to accommodate many substitutions on the ligand. The S pocket then widens onto the M, C1 and C2 pockets.

The active site viewer of Cerius2 was utilized for viewing, defining the active site pocket and for the purpose of de novo designing. LUDI analysis provided several new fragments for binding in the active site. New ligands generated from these fragments were minimized using semi-empirical AM1 method from the MOPAC interface available with sybyl7.1 software package. The protein-ligand interactions (both polar and non-polar) are then scored based on a scoring function which is an estimate of the free energy of binding (ΔG) of the protein-ligand complex. The scoring function used is a modification of the Böhm scoring function as described by Rarey et al [44].

Table 1 Docking scores of the reported inhibitors of NOS in the three isoforms

	Inhibitor	iNOS (4NOS)	eNOS (3NOS)	nNOS 1OM4)
1.	Lysine-4	−24.233	−10.505	−16.413
2.	Lysine-NIL	−23.053	−23.339	−28.617
3.	s-methyl homocitrulline	−22.422	−24.242	−24.672
4.	Fluorinated-l-lysine-14	−22.312	−23.484	−25.939
5.	Lysine-5	−22.205	−21.7	−24.99
6.	s-methyl-thiocitrulline	−21.656	−26.893	−28.421
7.	Fluorinated-l-lysine-4	−20.074	−24.314	−26.930
8.	2-azabicyclo-16	−19.802	−16.614	−14.341
9.	Lysine-10	−19.723	−24.428	−23.604
10.	s-butyl-thiocitrulline	−19.139	−18.285	−19.85
11.	Coumarin-37	−18.779	−6.378	−5.402
12.	Lysine-NMMA	−17.542	−19.857	−18.319
13.	2-iminopiperidines-8	−17.243	−17.332	−14.324
14.	Fluorinated-l-lysine-32	−17.144	−10.125	−14.411
15.	2-iminopyrrolidines-8	−16.918	−12.986	−12.834
16.	Lysines-GW274150	−16.692	−5.751	−15.198
17.	2-iminopyrrolidines-17	−16.666	−9.156	−15.532
18.	2-iminopyrrolidines-9	−16.069	−13.519	−13.34
19.	Tetrahydroazepin-16	−15.887	−15.705	−13.42
20.	Oxazol-3a	−15.163	−13.009	−12.686
21.	Coumarin-30	−15.136	−1.74	−
22.	s-ethyl-thiocitrulline	−15.002	−6.155	−14.347
23.	2-iminopyrrolidines-11	−14.981	−12.718	−
24.	2-iminopiperidines-17	−14.752	−16.005	−7.786
25.	2-iminopyrrolidines-13	−14.537	−10.332	−11.457
26.	2-iminopyrrolidines-6	−14.481	−13.635	−13.449
27.	Tetrahydroazepin-17	−14.189	−13.329	−14.838
28.	2-iminopiperidines-9	−14.064	−14.265	−12.151
29.	Oxazol-4a	−14.039	−12.119	−11.488
30.	2-iminopiperidines-11	−14.013	−12.851	−14.44
31.	Dihydropyr-2	−13.867	−14.668	−16.109
32.	Thiazol-14a-ES1537	−13.772	−12.841	−13.797
33.	Lysine-hNIL	−13.594	−13.698	−15.082
34.	2-azabicyclo-2	−13.519	−17.792	−16.030
35.	2-iminopyrrolidines-3	−13.377	−14.603	−9.708
36.	Dihydropyr-9	−13.359	−10.791	−10.560
37.	2-iminopyrrolidines-5	−13.108	−14.076	−15.588
38.	Oxazol-3b	−12.252	−13.061	−12.557
39.	Thiazol-14a	−12.209	−15.608	−12.951
40.	2-iminopyrrolidines-7	−12.090	−13.760	−13.341

Results and discussion

Fragment selection

a) Identification and selection of base fragments

An initial LUDI run with the default fragment library (available with Cerius2 software) comprising of about 1000 fragments gave 159 fragment hits. Most of them show (Fig. 2a) interactions with Trp372 and Glu377. These fragments were of similar framework as that of the already studied iNOS inhibitors reported in literature (Fig. 1), containing amidine, guanidine, thiourea motifs. However, no new fragments which maintain basic interactions with Trp372 and Glu377, were identified from the de novo analysis. This may be due to the absence of novel fragments in the fragment library of the software package. This prompted us to manually identify new motifs which may possess the internal structural similarity to the fragments showing the basic interactions. One common property noticed in already reported species as well as fragments identified from de novo analysis is the presence of the moieties I and II (Fig. 3). In most of the reported compounds as well as the fragments recognized from the LUDI analysis, there are two NH groups with a carbon linker which form hydrogen bonds with Trp372 and Glu377. The base interaction is due to these two N-H bonds with an intramolecular N-H——H-N distance of ~2.4–2.6 Å. The hypothesis employed during the manual search was to consider fragments with two NH_2 groups which maintain an intramolecular N-H——H-N distance similar to the fragments obtained from the LUDI analysis. NH_2 units which are separated by two sp^2 carbons show a similar distance (~2.4 Å) though the two NH_2 groups are not completely coplanar (Fig. 3). Such a relationship is not applicable when more than two linkers atoms are present between two NH_2 units as in 1,3-diaminobenzene (Fig. 3, IV). Hence, we focused our work on cyclic fragments with two adjacent NH_2 groups.

About 26 cyclic fragments with adjacent NH_2 groups were manually designed and entered into a LUDI library using the Genfra functionality for adding generic fragments. The de novo design run conducted using this user-specified library in the non-link mode showed that these fragments are quite suitable for binding in the cavity of NOSs. They form good hydrogen bonding with the Trp372 and Glu377 carbonyl oxygens to form the network as in Fig. 2b.

These findings were further supported by a molecular docking study (FlexX) of the same fragments into the active site with a binding pattern similar to the natural substrate, L-arginine. From the LUDI analysis as well as the FlexX analysis, it became clear that the fragment selection on the basis of two carbon atom linkers is viable. Some of the fragments chosen for this analysis are given in Fig. 4 along with their FlexX scores. The base fragment benzene-1,2-diamine was predicted to have the highest binding affinity

Table 2 The Total score, G score, PMF score, D score and Chem scores of the designed ligands and the reference molecule GW274150

Mol. Id	Total score			G score			PMF score			D score			Chem score		
	iNOS	ENOS	nNOS	iNOS	eNOS	nNOS	iNOS	eNOS	nNOS	iNOS	eNOS	nNOS	iNOS	eNOS	nNOS
M226	-24.21	NA	NA	-157.56	NA	NA	-124.69	NA	NA	-104.75	NA	NA	-33.15	NA	NA
M224	-21.31	-8.75	NA	-219.67	-171.48	NA	-117.48	-75.17	NA	-120.20	-102.69	NA	-35.81	-20.14	NA
M224a	-20.68	NA	NA	-154.78	NA	NA	-110.08	NA	NA	-102.25	NA	NA	-29.25	NA	NA
M226e	-21.52	NA	-16.60	-199.82	NA	-168.57	-109.87	NA	-88.61	-112.33	NA	-92.16	-31.56	NA	-25.04
M45	-20.0	NA	NA	-198.45	NA	NA	-98.71	NA	NA	-125.11	NA	NA	-40.06	NA	NA
M76	-30.33	-25.18	-21.26	-171.21	–	–	-119.08	–	–	-129.74	–	–	-40.52	–	–
M76d	-20.37	-6.38	-6.20	-196.79	-178.73	-177.35	-109.79	-87.28	-74.71	-123.18	-112.11	-115.46	-37.48	-32.96	-28.28
M76r	-29.30	-20.93	-8.51	-152.11	-142.74	-185.82	-110.60	-99.78	-111.94	-115.61	-99.13	-114.11	-39.57	-33.00	-33.65
M76f	-29.26	-16.60	-16.31	–	NA	–	–	NA	–	–	NA	–	–	NA	–
M27	-19.14	NA	-15.65	–	NA	–	–	NA	–	–	NA	–	–	NA	–
M7	-17.66	-3.57	NA	-167.99	–	NA	-69.86	–	NA	-83.93	–	NA	-30.43	–	NA
GW274150	-16.69	-5.75	-15.20	-60.31	–	26.89	-94.43	–	-88.21	-97.72	–	-84.69	-25.63	–	-20.78

NA: The molecule was not found in the docked solutions.

in both the LUDI and docking results with scores 343 (LUDI), -21.0 (FlexX), respectively. Figure 5 shows the interaction of this fragment in the heme active site. The base fragment also forms hydrogen bonding with Trp372 in addition to the bifurcated hydrogen bonding network with Glu377 in a similar manner to that of the substrate. R group substituents (Fig. 2b) can be added to any of the four free positions on the benzene ring of this fragment.

b) Defining side chain fragments

Once the base fragments are defined, the next step is to obtain the side chains for attachment to the base scaffold. The R group fragment library consisting of the side chains which are to be attached to the base scaffold was constructed by extracting the side chains of about 205 already reported iNOS inhibitors belonging to about 16 chemical classes like aminopyridine, 2-iminopyrrolidines, oxazolidine-2-imines, tetrahydro-2H-azepin-2-imines, 2-iminopiperidines, thiazo-lidine-2-imines, 2-aminothiazoles, coumarins, thienopyri-

dines, dihydropyridine-2(1H)-imines, azabicyclo-[4.1.0]-heptan-3-imines, 1,2-dihydro-4-quinazolinamines, 3,4-dihy-dro-1 isoquinolinamines, imidazopyridines, etc.

Focused library generation

Benzene-1,2-diamine was taken as the base fragment for further development of the ligand molecules, LUDI scores are considered as an important guide for predicting the binding affinity of the ligand to the target protein. A docking pose which includes H-bonding interactions with Trp372 and Glu377 is also an important criterion. The attachment points on this fragment for the various side chains obtained from the reported inhibitors are shown in Fig. 2b. The side chains were attached to the base scaffold by sketching followed by minimization of the molecules to generate a small focused library of around 226 ligand molecules.

Fig. 6 Structures of some of the ligands designed from the base fragment benzene-1,2- diamine
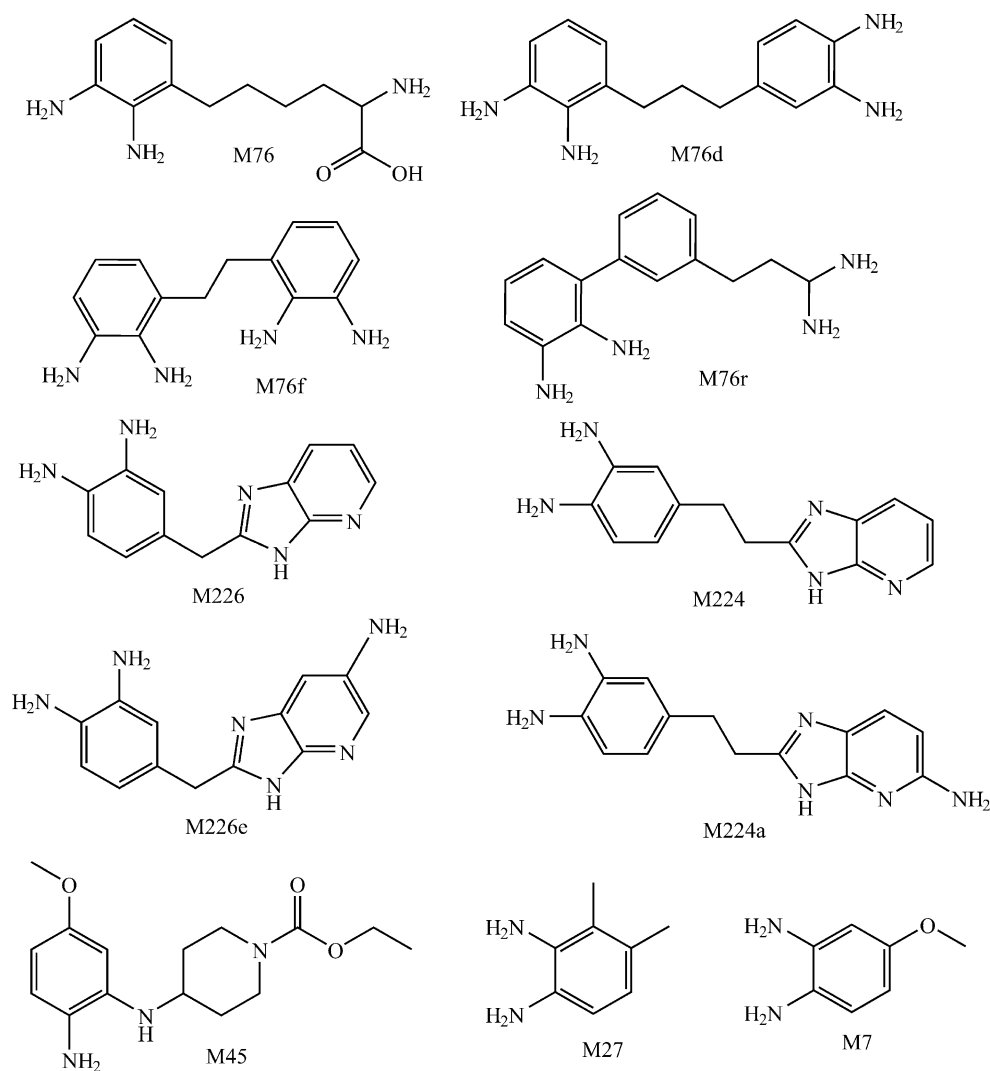
Docking analysis

The 226 molecules generated were initially docked into the active site of iNOS (PDB id: 4NOS) after manual definition of the active site comprised of about 38 residues including the heme. These were also similarly docked into the active site of eNOS (PDB id: 3NOS) and nNOS (PDB id: 1OM4). The binding affinities of these isoforms were estimated on the basis of relative binding scores. The scores for the reported molecules studied for NOS, which were used for the *in silico* validation of the designed molecules are given in Table 1.

Based on the docking results and the information obtained from the interaction sites given by LUDI, some of the ligands were modified further. The modification was carried out by visual inspection of the docking poses of the molecules in the active site so as to assign selective binding to iNOS. For example, molecule **M76** derived from a combination of the base fragment, benzene-1,2-diamine with that of the lysine side chain showed binding scores of −30.33 for iNOS, −25.18 for eNOS and −21.26 for nNOS. A decrease in binding scores for eNOS and nNOS was observed when the terminal moiety in **M76** was replaced with another benzene-1,2-diamine as in **M76d** and **M76f**. **M76r** also shows a reduction in binding scores but not so much for eNOS as for nNOS. Modifications on **M226** and **M224** also gave

molecules with stronger binding affinity towards iNOS than the other two isoforms like **M226e** and **M224a**. All the modified molecules also were added to the library and thus the size of the virtual library generated became 260 molecules. A comparative analysis of the docking scores in the three isoforms given by these designed ligands with that of an in-house database built from around 205 already reported inhibitors show that the docking scores of the designed ligands are comparable with that of the known inhibitors. Both the designed ligands and the reported inhibitors show highest docking scores around −30.0.

As a result of the docking analysis, an initial set of molecules were selected which showed comparatively good scores in iNOS but failed to show good docking scores towards eNOS and nNOS. The comparative binding scores of the designed molecules along with the reported iNOS selective inhibitor GW274150 for the three isoforms, iNOS, eNOS and nNOS are as shown in Table 2. All the ligands given in Fig. 6 show better binding scores than the reference ligand GW 274150, with respect to all scoring functions.

The docked conformation of one of the ligands, **M226** along with the reported inhibitor GW274150 in the active site is shown in Fig. 7. Molecules **M226**, **M224a**, **M45** failed to dock in eNOS and nNOS whereas they docked with a docking score of above -20.0 (FlexX) in iNOS. The other molecules showed somewhat less scores in eNOS and nNOS

Fig. 7 Figure shows the docked poses of the ligand M226 along with that of the reference GW274150. (FlexX analysis)
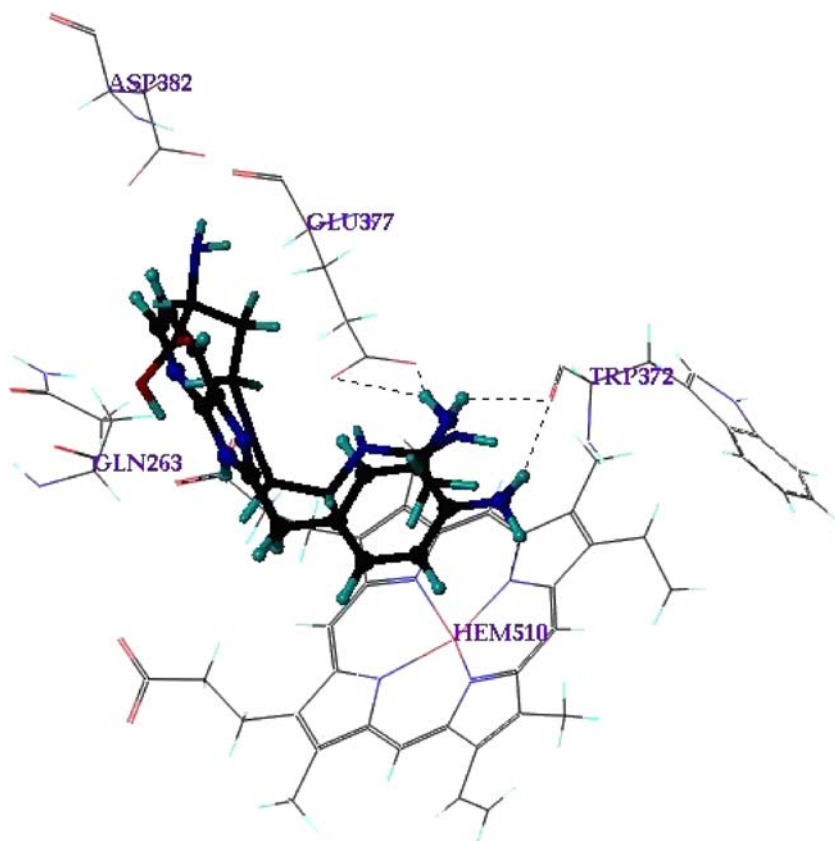
compared to that in iNOS. The structurally modified molecules **M76r** and **M76f** are predicted to have higher affinity towards iNOS, a corresponding increase is also shown in eNOS and nNOS, thus can not be considered selective.

The better binding scores of the designed ligands with iNOS in comparison to the reference ligand GW274150 can be attributed to increased flexibility of NH_2 groups in diaminobenzene moiety. In the already reported molecules (Fig. 1), the HN=C-NH_2 or related groups possess conjugative system and hence are less flexible. The two NH_2 groups on diamino-benzene unit are weakly conjugated with the benzene ring. These flexible NH_2 groups can form stronger H-bonding interactions with Trp372 and Glu377, whatever may be the special constraints on the rest of the molecule. The observed differences between the interactions noticed between the ligands in iNOS vs. eNOS and nNOS can be attributed to the residues Gln263 in iNOS. As shown in Fig. 7, Gln263 in iNOS plays an important role in binding with ligands, in nNOS and eNOS this amino acid is absent and thus leading to the observered trend in the ligand binding scores in iNOS vs. eNOS and nNOS. Thus, from the above analysis based on de novo design and molecular docking, we were able to identify some compounds which may show selective binding to iNOS.

Conclusions

Structure based drug design coupled with combinatorial library generation helps in generating focused libraries of compounds specifically for a single target rather than using a blanket approach of library generation. A combined de novo design and docking methodology was adopted to identify the base fragments which showed potential interactions with the main residues Trp372 and Glu377 involved in binding to the natural substrates in the S pocket of the heme active site in iNOS. A small focused combinatorial library was generated using the base fragment with the highest binding affinity (identified using LUDI analysis) and the side chains extracted from the already reported inhibitor molecules of NOS. The selectivity problem was addressed by comparative docking studies to the three isoforms of the NOS enzyme. The binding scores of each molecule was taken as the basis for selection. The satisfactory ligands screened out from the docking studies have a suitable balance of predictive binding affinity and predicted selectivities.

References

1. Kerwin Jr JF, Lancaster JR, Feldman PL (1995) J Med Chem 38:4343–4362
2. Hansen DW, Peterson KB, Trivedi M, Kramer SW, Webber RK, Tjoeng FS, Moore WM, Jerome GM, Kornmeier CM, Manning PT, Connor JR, Misko TP, Currie MG, Pitzele BS (1998) J Med Chem 41:1361–1366
3. Marletta MA (1994) J Med Chem 37:1899–1907
4. Knowles RG, Moncada S (1994) Biochem J 298:249–258
5. Crane BR, Arvai AS, Ghosh DK, Wu C, Getzoff ED, Stuehr DJ, Tainer JA (1998) Science 279:2121–2126
6. Crane BR, Arvai AS, Gachhui R, Wu C, Ghosh DK, Getzoff ED, Stuehr DJ, Tainer JA (1997) Science 278:425–431
7. Ji H, Li H, Flinspach M, Poulos TL, Silverman RB (2003) J Med Chem 46:5700–5711
8. Li H, Poulos TL (2005) J Inorg Biochem 99:293–305
9. Fischmann TO, Hruza A, Niu XD, Fossetta JD, Lunn CA, Dolphin E, Prongay AJ, Reichert P, Lundell DJ, Narula SK, Weber PC (1999) Nat Struct Biol 6:233–242
10. Li H, Raman CS, Glaser CB, Blasko E, Young TA, Parkinson JF, Whitlow M, Poulos TL (1999) J Biol Chem 274:21276–21284
11. Fedorov R, Vasan R, Ghosh DK, Schlichting I (2004) Proc Natl Acad Sci USA 101:5892–5897
12. Alderton WK, Cooper CE, Knowles RG (2001) Biochem J 357:593–615
13. Olken NM, Marletta MA (1993) Biochemistry 32:9677–9685
14. Furfine ES, Harmon MF, Paith JE, Garvey EP (1993) Biochemistry 32:8512–8517
15. McCall TB, Feelisch M, Palmer RM, Moncada S (1991) Br J Pharmacol 102:234–238
16. Babu BR, Griffith OW (1998) J Biol Chem 273:8882–8889
17. Narayanan K, Griffith OW (1994) J Med Chem 37:885–887
18. Moore WM, Webber RK, Jerome GM, Tjoeng FS, Misko TP, Currie MG (1994) J Med Chem 37:3886–3888
19. Misko TP, Moore WM, Kasten TP, Nickols GA, Corbett JA, Tilton RG, McDaniel ML, Williamson JR, Currie MG (1993) Eur J Pharmacol 233:119–125
20. Garvey EP, Oplinger JA, Tanoury GJ, Sherman PA, Fowler M, Marshall S, Harmon MF, Paith JE, Furfine ES (1994) J Biol Chem 269:26669–26676
21. Southan GJ, Szabo C, Thiemermann C (1995) Br J Pharmacol 114:510–516
22. Moore WM, Webber RK, Fok KF, Jerome GM, Connor JR, Manning PT, Wyatt PS, Misko TP, Tjoeng FS, Currie MG (1996) J Med Chem 39:669–672
23. Hagen TJ, Bergmanis AA, Kramer SW, Fok KF, Schmelzer AE, Pitzele BS, Swenton L, Jerome GM, Kornmeier CM, Moore WM, Branson LF, Connor JR, Manning PT, Currie MG, Hallinan EA (1998) J Med Chem 41:3675–3683
24. Beaton H, Boughton-Smith N, Hamley P, Ghelani A, Nicholls DJ, Tinker AC, Wallace AV (2001) Bioorg Med Chem Lett 11:1027–1030
25. Beaton H, Hamley P, Nicholls DJ, Tinker AC, Wallace AV (2001) Bioorg Med Chem Lett 11:1023–1026
26. Tinker AC, Beaton HG, Boughton-Smith N, Cook TR, Cooper SL, Fraser-Rae L, Hallam K, Hamley P, McInally T, Nicholls DJ, Pimm AD, Wallace AV (2003) J Med Chem 46:913–916
27. Connolly S, Aberg A, Arvai A, Beaton HG, Cheshire DR, Cook AR, Cooper S, Cox D, Hamley P, Mallinder P, Millichip I, Nicholls DJ, Rosenfeld RJ, St-Gallay SA, Tainer J, Tinker AC, Wallace AV (2004) J Med Chem 47:3320–3323
28. Kawanaka Y, Kobayashi K, Kusuda S, Tatsumi T, Murota M, Nishiyama T, Hisaichi K, Fujii A, Hirai K, Naka M (2003) Bioorg Med Chem 11:1723–1743
29. Kawanaka Y, Kobayashi K, Kusuda S, Tatsumi T, Murota M, Nishiyama T, Hisaichi K, Fujii A, Hirai K, Nishizaki M, Naka M, Komeno M, Nakai H, Toda M (2003) Bioorg Med Chem 11:689–702
30. Ueda S, Terauchi H, Kawasaki M, Yano A, Ido M (2004) Chem Pharm Bull 52:634–637

31. Ueda S, Terauchi H, Yano A, Ido M, Matsumoto M, Kawasaki M (2004) Bioorg Med Chem Lett 14:313–316
32. Ueda S, Terauchi H, Yano A, Matsumoto M, Kubo T, Kyoya Y, Suzuki K, Ido M, Kawasaki M (2004) Bioorg Med Chem 12:4101–4116
33. Ueda S, Terauchi H, Suzuki K, Yano A, Matsumoto M, Kubo T, Minato H, Arai YT, Suji J, Watanabe N (2005) Bioorg Med Chem Lett 15:1361–1366
34. Strub A, Ulrich WR, Hesslinger C, Eltze M, Fuchss T, Strassner J, Strand S, Lehner MD, Boer R (2006) Mol Pharmacol 69:328–337
35. Naka M, Nanbu T, Kobayashi K, Kamanaka Y, Komeno M, Yanase R, Fukutomi T, Fujimura S, Seo HG, Fujiwara N, Ohuchida S, Suzuki K, Kondo K, Taniguchi N (2000) Biochem Biophys Res Commun 270:663–667
36. Young RJ, Beams RM, Carter K, Clark HA, Coe DM, Chambers CL, Davies PI, Dawson J, Drysdale MJ, Franzman KW, French C, Hodgson ST, Hodson HF, Kleanthous S, Rider P, Sanders D, Sawyer DA, Scott KJ, Shearer BG, Stocker R, Smith S, Tackley MC, Knowles RG (2000) Bioorg Med Chem Lett 10:597–600
37. Salerno L, Sorrenti V, Di Giacomo C, Romeo G, Siracusa MA (2002) Curr Pharm Des 8:177–200
38. Babu BR, Frey C, Griffith OW (1999) J Biol Chem 274:25218–25226
39. Aparna V, Desiraju G.R, Gopalakrishnan B (2007) J Mol Graph Model 26:457–470
40. Haitao Ji, Gomez-Vidal, Jose A, Martasek P, Roman LJ, Silverman, RB (2006) J Med Chem 49:6254–6263
41. Seo J, Igarashi J, Li H, Martasek P, Roman LJ, Poulos TL, Silverman RB (2007) J Med Chem 50:2089–2099
42. David DD, Adler M, Arnaiz D, Eagen K, Erickson S, Guilford W, Kenrick, M, Morrissey MM, Ohlmeyer M, Pan G, Paradkar VM, Parkinson J, Polokoff M, Saionz K, Santos C, Subramanyam B, Vergona R, Wei RG, Whitlow M, Ye B, Zhao Z, Devlin JJ, Phillips G (2007) J Med Chem 50:1146–1157
43. Bohm HJ (1994) J Comput Aided Mol Des 8:243–256
44. Rarey M, Kramer B, Lengauer T, Klebe G (1996) J Mol Biol 261:470–489